ASIA-PACIFIC SOLAR RESEARCH CONFERENCE

PEER REVIEWED
ASIA-PACIFIC
SOLAR RESEARCH CONFERENCE



# Diffuse Solar Potential of Facades in an Urban Context under Different Sky Conditions

Naveed ur Rehman[1], Timothy Anderson[1] and Roy Nates[1]

[1]*Department of Mechanical Engineering, Auckland University of Technology, Auckland, New Zealand*

*E-mail: timothy.anderson@aut.ac.nz*

## Abstract

This paper presents an advance in a method to evaluate the diffuse solar potential on facades in the urban environment. The proposed method is suitable to work in both the isotropic and anisotropic sky conditions. It employs the 2.5D geo-information model, combined with the forward ray-tracing technique that has been found efficient in urban analysis due to its hyperpoint-independent characteristic. For the anisotropic sky conditions, a well-known solar radiance model is integrated to include the atmosphere-dependent scenarios by considering the solar diffuse fraction, clearness index and the position of sun in the sky. To illustrate this work, an urban case study performed under various sky conditions is presented. The results obtained are compared and discussed.

## 1. Introduction

In recent times it has been recognised that the façades of tall and slender buildings that exist in modern cities offer significantly more scope for installing the solar devices than their roofs (Freitas, et al., 2015). Unfortunately, not all façades receive the same amount of solar radiation due to the sun's trajectory across the day. Added to this, in complex urban settings, the shadows and sky-blockings of the nearby urban and natural features may further limit the availability of solar radiation at the desired locations. This eventually complicates the development of models for quantifying solar availability on building surfaces.

In this vein, numerical solar potential models that make use of 2.5D geo-information models (GIMs) have been developed (Hofierka, et al., 2002; Wiginton, et al., 2010). However, most of these models are not applicable for producing trustworthy estimates on vertical surfaces (Carneiro, et al., 2010). The main reason for this limitation is the basic design of these models in that they use a "point-to-sky" (or backward ray-tracing) approach. This makes it practically impossible for them to assess and store the results for, what is, effectively an infinite number of points (called *hyperpoints*) on the façade.

Having identified the scarcity of reliable methods in this genre, the authors recently proposed a hyperpoint-independent algorithm that uses a "sky-to-point" (or forward ray-tracing) approach (Rehman, et al., 2016; Rehman, et al., 2017). This method utilizes several spatially-scaled GIMs and the temporally-scaled solar irradiation model to assess the direct solar radiation potential in a given period. A unique shadow algorithm was also illustrated to be easily converted into a computer program in which the time and computer memory required for the assessment was independent of the complexity of a given relief.

This work presents the results of the model (Rehman, et al., 2016; Rehman, et al., 2017) when it is used to evaluate the diffuse solar potential on façades, for anistropic sky

conditions, through the integration of a well-known solar radiance model proposed by Brunger and Hooper (Brunger and Hooper, 1993).

## 2. Method

The diffuse solar potential is generally expressed as the ratio between the available diffuse irradiance received at a point on a tilted surface ($D_T$, W/m$^2$) and the total diffuse irradiance received on the horizontal surface under unobstructed sky ($D$, W/m$^2$). Whereas, the irradiance can be considered as the accumulation of radiances (rays) approaching to a point from all over the sky. As long as the magnitude of these radiances is uniform throughout the sky (isotropic), the ratio can be of geometric nature. In literature, it is more commonly pronounced as Sky View Factor (SVF), describing the fraction of sky visible from the point. However, under the anisotropic sky conditions, where the situation is more complicated due to the varying magnitude of radiances over the sky, the SVF does not seem to adequately explain the conceptual understanding of diffuse solar potential. Hence, in order to generalize the thought of diffuse solar potential in both types of sky conditions, the term Diffuse Solar Factor (DSF) has been used here which can mathematically be defined as:

$$DSF = D_T/D \quad \textbf{(1)}$$

In the context of this work, $D_T$ is measured at the façadal points of urban structures, surrounded by other buildings obstructing the radiances approaching from the visible sky view. The value of $D_T$ can be obtained by utilizing the technique of discretizing the celestial sky vault (Rehman and Siddiqui, 2015), such that:

$$D_T = \sum_{\gamma_e=0^\circ}^{360^\circ} \sum_{\alpha_e=0^\circ}^{90^\circ} R.i.\omega.V \quad \textbf{(2)}$$

where $R$ (W/m$^2$.sr) is the radiance approaching from a sky element located at ($\gamma_e$,$\alpha_e$) as shown in Figure 1. $i$ is the incidence factor that depends upon the cosine of the angle between the normal of the façade at the point and the direction of radiance. $\omega = \cos\alpha_e \, \Delta\gamma_e \Delta\alpha_e$ is the solid angle associated with the sky element and $V$ is the visibility factor which holds the information about whether the point can see the sky in the direction of the radiance or not. This factor can be obtained by executing the authors previously proposed shadow algorithm (Rehman, et al., 2017), taking the lines-of-scan of a 2.5D geo-information model, one by one, in the direction of each sky element.

On the other hand, $D$ in Eq. (1) is estimated at an unobstructed site on the horizontal and thus remains constant throughout. Mathematically:

$$D = \sum_{\gamma_e=0^\circ}^{360^\circ} \sum_{\alpha_e=0^\circ}^{90^\circ} R.sin\alpha_e.\omega \quad \textbf{(3)}$$

For the isotropic sky condition, the radiances approaching from all the elements are equal. Hence, the radiance term ($R$) should be treated as constant in the expressions of $D_T$ (Eq. (2)) and $D$ (Eq. (3)). So, simplifying Eq. (1) for the isotropic sky condition yields the expression of DSF, such that:

$$DSF = \frac{\sum_{\gamma_e=0^\circ}^{360^\circ} \sum_{\alpha_e=0^\circ}^{90^\circ} i.\omega.V}{\sum_{\gamma_e=0^\circ}^{360^\circ} \sum_{\alpha_e=0^\circ}^{90^\circ} sin\alpha_e.\omega} \quad \textbf{(4)}$$

However, when the sky is anisotropic, the incoming diffuse radiance is composed of three components, each having its dominance at different sky regions. The first is the isotropic diffuse component which is received equally from all elements. The other is the horizon

brightening component which is concentrated near horizon and most pronounced in clear skies with unobstructed views. The last is the circumsolar diffuse component which is concentrated in the region of the sky around the sun (Duffie and Beckman, 2013).

In other words, the radiance approaching from each element of the sky should be accounted distinctly i.e. $R = R_{aniso}(\alpha_e, \gamma_e)$. The magnitude of these radiances as the angular position of their associated sky element can be obtained by the Brunger and Hooper model (Brunger and Hooper, 1993), given by:

$$R_{aniso}(\alpha_e, \gamma_e) = D\left[\frac{a_o + a_1 \cos\theta + a_2 \exp(-a_3\psi)}{\pi(a_o + 2a_1/3) + 2a_2 I(90 - \alpha_s, a_3)}\right] \quad \textbf{(5)}$$

where in numerator, the first term (constant) represents the isotropic diffuse component, the term proportional to the $\cos\theta$ takes into account the horizon brightening component and the circumsolar component is modeled as an exponential decay as it decreases rapidly with angular distance from the solar disk.

In Eq. (5), the assignable values for the parameters $a_0$, $a_1$, $a_2$ and $a_3$ that allow the sky radiance model to respond to the atmospheric radiation conditions are tabulated in Table 2 of ref. (Brunger and Hooper, 1993). These values are specified in the form of range for solar diffuse fraction ($k$) and the atmospheric clearness index ($k_t$). The value of $k$ represents the fraction of diffuse component in the global irradiance. So, under the overcast sky condition, when most of the incoming irradiance is diffuse in nature, the value of $k$ is high (close to 1). Whereas, under the clear sky condition, when the direct component is more dominant than the diffuse component, the value of $k$ is low (close to 0). Note that, under clear skies, the circumsolar diffuse is weighted more heavily than the isotropic diffuse. On the other hand, the value of $k_t$ describes the fraction of global irradiance in extra-terrestrial irradiance. The main reason of attenuation of global irradiance is its scattering and absorbing in the atmosphere. Hence, an overcast sky corresponds to a low value of $k_t$ (close to 0) compared with the clear sky, which represents a high value of $k_t$ (close to 1). The partly cloudy sky condition has an average value of $k$ and $k_t$ (close to 0.5).

$\psi$(rad) in Eq. (5), is the angle between the direction of element and the sun, given by Eq. (), and $I$ is given by Eq. ().

$$\psi(90 - \alpha_e, \gamma_e) = \cos^{-1}(\cos\alpha_e \cos\alpha_s \cos(\gamma_e - \gamma_s) + \sin\alpha_e \sin\alpha_s) \quad \textbf{(6)}$$

$$I(90 - \alpha_s, a_3) = \frac{[1 + \exp(-a_3\pi/3)]}{a_3^{2+} + 4} \times \left\{\pi - \left[1 - \frac{2[1 - \exp(-a_3\pi)]}{\pi a_3[1 + \exp(-a_3\pi/2)]}\right] \times \left[\frac{\pi(90 - \alpha_s)\cos\alpha_s}{90} - 0.02\pi \sin\big(2(90 - \alpha_s)\big)\right]\right\} \quad \textbf{(7)}$$

where $\alpha_s$ and $\gamma_s$ are the altitude and azimuth angle of sun.

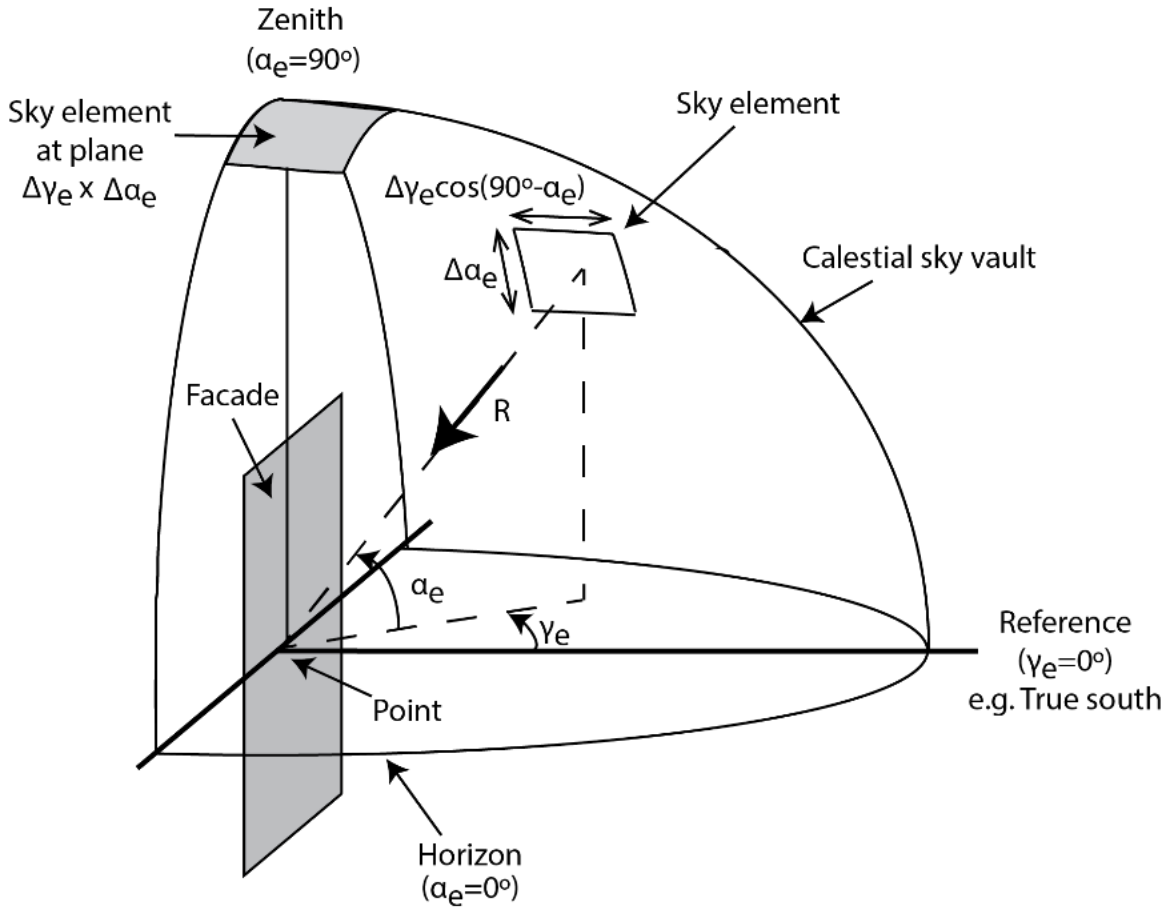


**Figure 1. The sky vault around the point on façade**

To demonstrate the proposed method a hypothetical layout located in Auckland (New Zealand) was chosen for analysis, as shown in Figure 2 (Rehman, et al., 2017). The scene consists of three buildings (A, B and C) of different heights, each having four façades.

For simulating an isotropic sky condition, only the mathematical relations as given in Eqs. (1)-(3) were utilized. Whereas, for the anisotropic sky conditions, the desired parameters associated with the sky conditions and the sun position were obtained from a typical weather year file (University of Wisconsin, 2010) and Brunger and Hooper (1993), as listed in Table I. To obtain a fair comparison, the times in the year for each condition were selected to ensure that the sun was at the same position.

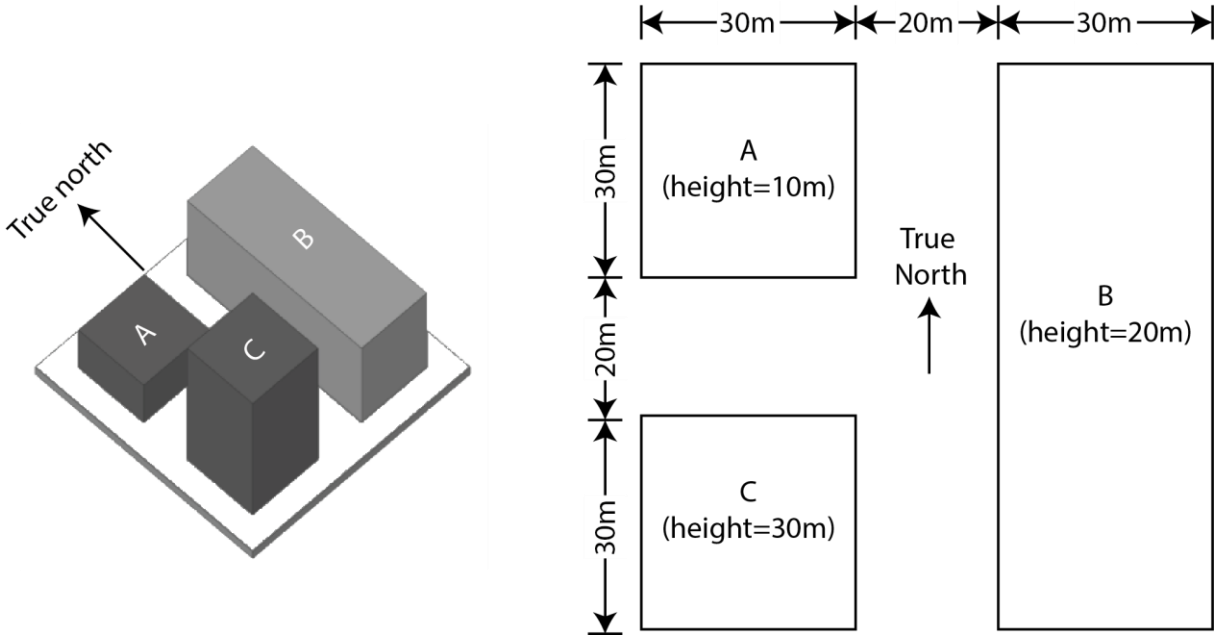


**Figure 2. Hypothetical layout put up for the simulation and analysis purposes (Rehman, et al., 2017)**

**Table I. Simulation parameters for the different anisotropic sky conditions**

| Simulation parameters | Clear sky | Partly cloudy sky | Overcast sky |
|---|---|---|---|
| **Time of year (hr)** | 1214 | 1406 | 1118 |
| $k$ | 0.25 | 0.55 | 0.95 |
| $k_t$ | 0.75 | 0.55 | 0.05 |
| $a_o$ | 0.3071 | 0.2465 | 0.1864 |
| $a_1$ | -0.2576 | -0.1245 | 0.1979 |
| $a_2$ | 2.3127 | 2.9163 | 0.0000 |
| $a_3$ | 3.5189 | 4.0760 | 1.0000 |
| **Sun azimuth angle ($\gamma_S$)** | 29.2° NW | 27.37° NW | 30.31° NW |
| **Sun altitude angle ($\alpha_S$)** | 61.36° | 58.55° | 62.66° |

## 3. Results and Discussion

The DSF at the highest points of the building “A” on the façade facing north are shown in Figure 3. For this façade, the view to the sky and sun is not obstructed by any other object (or building) resulting in it having a constant DSF. The value of DSF for the isotropic sky condition is found to be 50%, which corresponds with the result for vertical façades by other analytical models (Liu and Jordan, 1961). The clear and the partly cloudy sky yielded the highest DSF, ranging between 57-58%. This is because of the strong influence of circumsolar diffuse component, depicted by the low value of $k$ as well as high incidence factor associated with the sky elements around sun position. The DSF for the overcast sky condition is found to be lowest among all other conditions (approximately 43%).

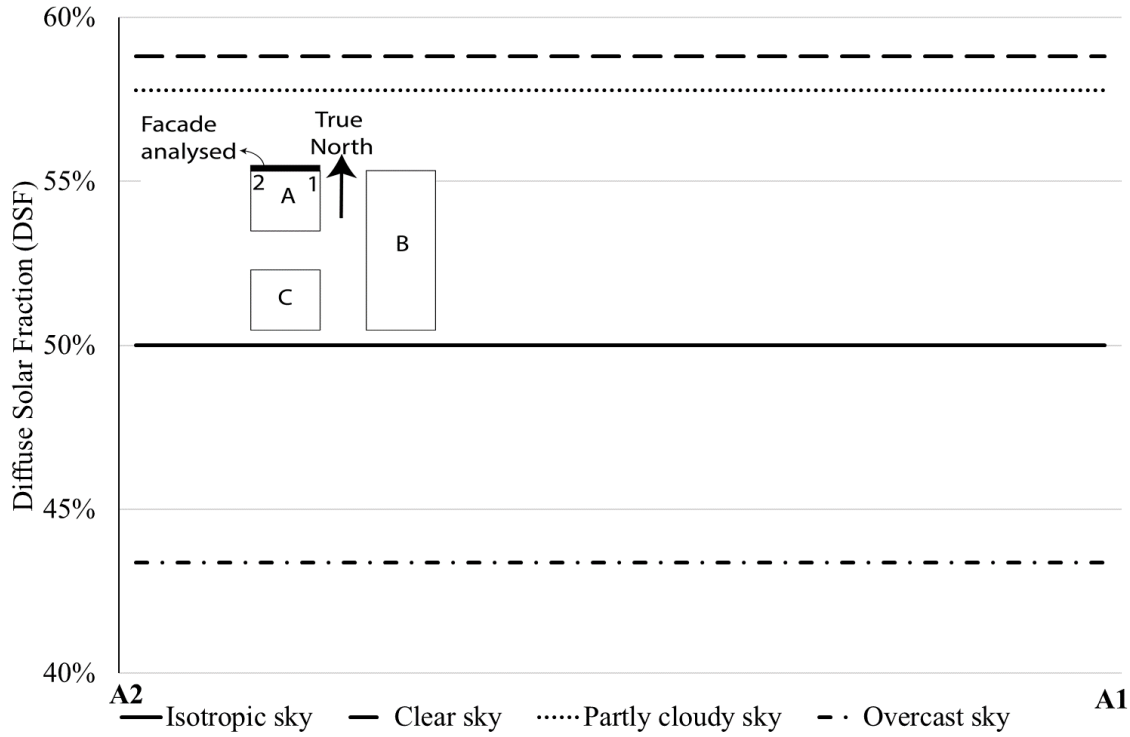


**Figure 3: Diffuse solar fraction at the highest points of building "A" on the north facing façade**

The DSF at the highest points of the building "B" on the façade facing west are shown in Figure 4. The sky view of this façade is obstructed by the building "C" and is unique at every point (Figure 5). For example, the points which are closer to this building receives largely obstructed sky (e.g. at or near front) compared to the points which are far (e.g. at or near northern corner). On the other hand, the façade is able to see the sun from all the points, and hence can receive the circumsolar diffuse component. But unlike the northern façade of building "A", the incidence effect is poor as the façade normal is facing west and the sun is near north. Hence, the overall contribution of the circumsolar component is not very influential. The DSF for the isotropic sky condition falls between 25-45%. As was expected, it has its higher values near northern corner and the minimum values at the points near and at front of building "C". As the view to the sky plays a significant role in receiving the radiances, the DSF in isotropic and all the anisotropic sky conditions is following the similar trend. The DSF in clear sky condition is slightly higher than for the isotropic sky because of the circumsolar component. However, the DSF of the partly cloudy sky condition is found very close to the isotropic sky condition. The overcast sky condition yielded the lowest DSF among others.

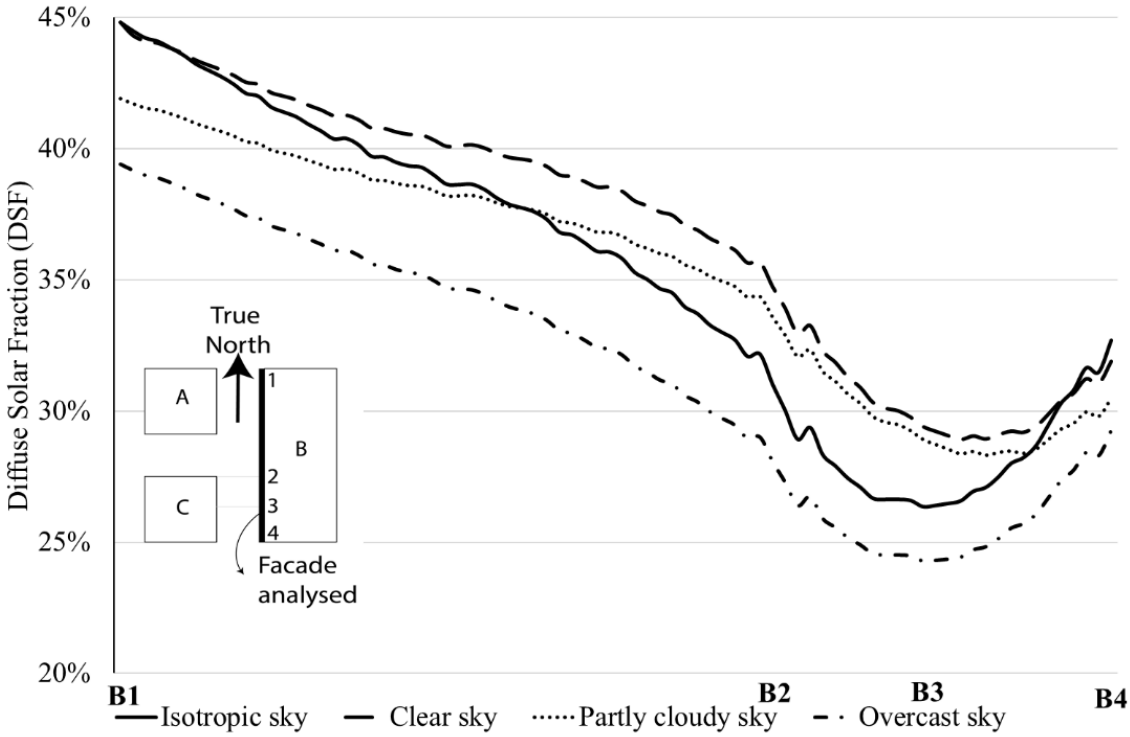


**Figure 4. Diffuse solar fraction at the highest points of building "B" on the west facing façade**

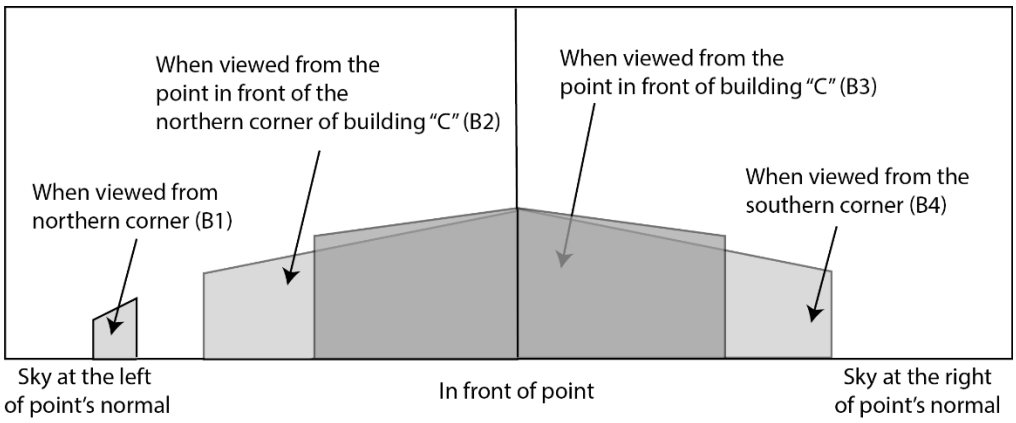


**Figure 5. The sky view obstructed by Building C when seen from the different points at Building B**

## 4. Conclusion

With this improvement of our existing method (Rehman, et al., 2016; Rehman, et al., 2017), the model can now be used to evaluate the diffuse solar potential on façades in an urban environment. The ability to do so is represented by factor named DSF, which is the available diffuse solar irradiance received at the point on the façade normalized to the diffused irradiance received at horizontal under unobstructed sky. The proposed method is suitable to work in both the isotropic and anisotropic sky conditions as it can respond to the atmosphere-dependent scenarios by taking into account the solar diffuse fraction, clearness index and the position of sun in sky. For the anisotropic sky conditions, the integration of the well-known solar radiance model proposed by Brunger and Hooper (Brunger and Hooper, 1993) was demonstrated.

For the analysis, a case study considering a hypothetical building layout, situated in Auckland (New Zealand) was presented. The information related to the solar irradiance and position were obtained from the TRNSYS software tool. The simulations were performed to yield the diffuse solar potential of façades. The two different façades in the layout were analyzed. The façade which was facing north with an unobstructed sky was found to have constant DSF. Whereas, the façade which was facing west and its sky view was obstructed by another building was found to have DSF varied over its length. The contribution of the visibility of the sky and the influence of circumsolar component together with the incidence effects of its associated sky elements, found to have significant effect on the DSF.

The authors have demonstrated the forward ray tracing as a useful approach for assessing the direct (Rehman, et al., 2017) and diffuse solar potential at façades. As in this approach, the rays are traced along their path, this characteristic can also be utilized for analyzing the direct and diffuse reflections from the urban objects and the ground (albedo). Also, when these models are combined with the performance models of solar technologies, they can help in predict very useful information in which the end-users are generally interested in e.g. the power output from PV panels and production of hot water from thermal collectors etc.

**References**

Brunger, A. and Hooper, F., 1993, 'Anisotropic sky radiance model based on narrow field of view measurements of shortwave radiance', *Solar Energy*, 51(1), p53-64.

Carneiro, C., Morello, E., Desthieux, G. and Golay, F, 2010, 'Urban environment quality indicators: application to solar radiation and morphological analysis on built area' *Proceedings of the 3rd WSEAS international conference on visualization, imaging and simulation*, p141-148.

Duffie, J. A. and Beckman, W. A., 2013, 'Solar engineering of thermal processes', *Wiley New York*, 3rd ed.

Freitas, S., Catita, C., Redweik, P. and Brito, M, 2015, 'Modelling solar potential in the urban environment: State-of-the-art review', *Renewable and Sustainable Energy Reviews*, 41, p915-931.

Hofierka, J. and Suri, M, 2002. 'The solar radiation model for Open source GIS: implementation and applications', *Proceedings of the Open source GIS-GRASS users conference*, p51-70.

Liu, B. and Jordan, R., 1961, 'Daily insolation on surfaces tilted towards equator', *ASHRAE Transactions*, 67, p526–541.

Rehman, N. U., Anderson, T. and Nates, R, 2016, 'Solar Potential Assessment of Façades s in an Urban Context: An Algorithm for 1.5D Digital Surface Models' *Asia-Pacific Solar Research Conference, Canberra*, p1-8.

Rehman, N. U., Anderson, T. and Nates, R, 2017, 'Solar Potential Assessment of Façades s in an Urban Context: An Algorithm for 2.5D Digital Surface Models' *Asia-Pacific Solar Research Conference, Melbourne*, p1-9.

Rehman, N. U., and Siddiqui, M. A, 2015, 'A novel method for determining sky view factor for isotropic diffuse radiations for a collector in obstacles-free or urban sites' *Journal of Renewable and Sustainable Energy*, 7(3), 033110.

University of Wisconsin, 2010, 'TRNSYS 17: A transient system simulation program' *Solar Energy Laboratory*.

Wiginton, L., Nguyen, H., and Pearce, J, 2010, 'Quantifying rooftop solar photovoltaic potential for regional renewable energy policy' *Computers, Environment and Urban Systems*, 34(4), p345-357.